Novel Innate Immune Genes Regulating the Macrophage Response to Gram Positive Bacteria

Scott Alper,*,†,‡ Laura A. Warg,‡ Lesly De Arras,†,‡ Brenna R. Flatley,*,† Elizabeth J. Davidson,†,§ Jenni Adams,† Keith Smith,§ Christine L. Wohlford-Lenane, Paul B. McCray, Jr.,** Brent S. Pedersen,§ David A. Schwartz,†,‡,§ and Ivana V. Yang†,§,††,1**

*Department of Biomedical Research and †Center for Genes, Environment, and Health, National Jewish Health, Denver, Colorado 80206, ‡Department of Immunology and Microbiology and §Department of Medicine, University of Colorado Anschutz Medical Campus, and ††Department of Epidemiology, Colorado School of Public Health, University of Colorado Denver, Aurora, Colorado 80045, and **Department of Pediatrics, Carver College of Medicine, University of Iowa, Iowa City, Iowa 52242

ABSTRACT Host variation in Toll-like receptors and other innate immune signaling molecules alters infection susceptibility. However, only a portion of the variability observed in the innate immune response is accounted for by known genes in these pathways. Thus, the identification of additional genes that regulate the response to Gram positive bacteria is warranted. Bone marrow-derived macrophages (BMMs) from 43 inbred mouse strains were stimulated with lipotechoic acid (LTA), a major component of the Gram positive bacterial cell wall. Concentrations of the proinflammatory cytokines IL-6, IL-12, and TNF-α were measured. *In silico* whole genome association (WGA) mapping was performed using cytokine responses followed by network analysis to prioritize candidate genes. To determine which candidate genes could be responsible for regulating the LTA response, candidate genes were inhibited using RNA interference (RNAi) and were overexpressed in RAW264.7 macrophages. BMMs from Bdkrb1-deficient mice were used to assess the effect of Bdkrb1 gene deletion on the response to LTA, heat-killed *Streptococcus pneumoniae*, and heat-killed *Staphylococcus aureus*. WGA mapping identified 117 loci: IL-6 analysis yielded 20 loci (average locus size = 0.133 Mb; 18 genes), IL-12 analysis produced 5 loci (0.201 Mb average; 7 genes), and TNF-α analysis yielded 92 loci (0.464 Mb average; 186 genes of which 46 were prioritized by network analysis). The follow-up small interfering RNA screen of 71 target genes identified four genes (*Bdkrb1*, *Blnk*, *Fbxo17*, and *Nkx6-1*) whose inhibition resulted in significantly reduced cytokine production following LTA stimulation. Overexpression of these four genes resulted in significantly increased cytokine production in response to LTA. Bdkrb1-deficient macrophages were less responsive to LTA and heat-killed *S. aureus*, validating the genetic and RNAi approach to identify novel regulators of the response to LTA. We have identified four innate immune response genes that may contribute to Gram positive bacterial susceptibility.

KEYWORDS innate immunity; Gram positive bacteria; lipotechoic acid; whole genome association mapping; inbred strains of mice; RNA interference

GRAM positive bacterial infections are a major public health concern, with pneumonia for example, being the most prevalent lower respiratory infection and third leading cause of death around the world (Liu *et al.* 2015). Around 10% of healthy adults and 20–40% of healthy children have airways colonized by the most common pneumonia pathogen, *Streptococcus pneumoniae* (van der Poll and Opal 2009) but only a small portion of these individuals become actively infected (Brouwer *et al.* 2009). Similarly, the rate of *Staphylococcus aureus* infection is high in hospitals and community settings. However, animal and human studies have shown variable host response and course of disease (Shukla *et al.* 2015), suggesting genetic factors in the innate immune response to the pathogen are likely at play.

The innate immune response begins with binding of the pathogen-associated molecular pattern (PAMP) to innate immune receptors such as the Toll-like receptor (TLR) (Takeuchi and Akira 2010) and nucleotide-binding domain, leucine rich containing (NLR) (Ting *et al.* 2008) families. In particular, the TLR2/TLR6 heterodimer on cell surfaces binds to peptidoglycan and the lipotechoic acid (LTA) moieties of

doi: 10.1534/genetics.115.185314
Manuscript received November 24, 2015; accepted for publication June 19, 2016; published Early Online June 28, 2016.
Supplemental material is available online at www.genetics.org/lookup/suppl/doi:10.1534/genetics.115.185314/-/DC1.
[1]Corresponding author: Department of Medicine, University of Colorado Denver, 12700 E. 19th Ave., 8611, Aurora, CO 80045. E-mail: ivana.yang@ucdenver.edu

Gram positive bacteria, initiating a signaling cascade that leads to activation of NF-κB and production of proinflammatory cytokines.

Novel genes involved in the innate immune response to a variety of PAMPs and pathogens have been identified by our group using comparative genomics approaches (Alper *et al.* 2008), transcriptional profiling of stimulated macrophages (Yang *et al.* 2011b) and tissues from animal models (Yang *et al.* 2011a), and mapping studies in inbred mice (Zaas *et al.* 2008; Yang *et al.* 2009). A prior study from our laboratory investigated murine antibacterial defense to streptococcal lung infection in eight strains of mice and found that TLR2-deficient mice had increased bacterial load (Hollingsworth *et al.* 2007), and a similar study in nine inbred mouse strains identified resistant and susceptible strains of mice (Gingles *et al.* 2001). To date, no study has examined the cytokine response to TLR2 stimulation, either *in vitro* or *in vivo*, on a genome-wide scale across a larger number of mouse strains. Here, we use inbred mouse strains and subsequent loss- and gain-of-function approaches to identify novel regulators of the response to the TLR2/6 PAMP LTA.

Materials and Methods

Animals

Inbred mouse strains were obtained from The Jackson Laboratory (Bar Harbor, ME) and killed for collection of bone marrow. Bdkrb1-deficient mice were created by Michael Bader (Pesquero *et al.* 2000). Three mice per strain were used. All animal work was reviewed and approved by the Institutional Animal Care and Use Committees at National Jewish Health and the University of Colorado Anschutz Medical Campus.

Bone marrow-derived macrophage culture

Bone marrow-derived macrophages (BMMs) were generated *in vitro* using standard methodology (Weischenfeldt and Porse 2008). Briefly, bone marrow was harvested from the femurs and tibia, disaggregated, washed, and resuspended in DMEM medium supplemented with 4,500 mg/liter of D-glucose, L-glutamine, 110 mg/liter of sodium pyruvate (high glucose medium; Invitrogen, Carlsbad, CA), 10% heat-inactivated FCS, 100 units/ml penicillin, 100 μg/ml streptomycin (all from Invitrogen), and 25 ng/ml recombinant mouse M-CSF (R&D Systems, Minneapolis, MN). Ten milliliters of this suspension was plated in each of two Petri dishes and cultured at 37° in a 5% CO_2 incubator for 6 days. On day 6, nonadherent contaminating cells were removed by three PBS washes. Washed cells were replated at 5×10^5 per well in 96-well plates and incubated at 37° overnight. Following overnight incubation, the cells were stimulated with three concentrations of *S. aureus* LTA (Sigma, St. Louis, MO) (10, 0.5, and 0.025 μg/ml) in duplicate. Three biological replicates (*i.e.*, three mice per strain) were included. Supernatant was collected 5 hr post-PAMP treatment and cytokine production (IL-6, IL-12p40, and TNF-α) was assayed using the Bio-Plex Kit (Bio-Rad, Hercules, CA) and read on a Luminex reader (Bio-Rad).

Whole genome association mapping analysis

Cytokine concentrations were $\log_{10}$ transformed, duplicate readings for each mouse were averaged, and all further data analysis was performed using triplicate biological replicates. Normality of distribution of cytokine response was assessed using the D'Agostino–Pearson omnibus normality test (GraphPad Prism) and the concentration with the most normally distributed data (0.5 μg/ml) was used for mapping. *In silico* whole genome association (WGA) mapping was conducted using efficient mixed model association (EMMA) (Kang *et al.* 2008) using the 4 million SNP data set to identify genetic loci associated with cytokine production in response to LTA stimulation. EMMA corrects for population structure and relatedness between inbred mouse strains using a phylogenetic kinship matrix to avoid false positive associations. We also performed permutation testing with shuffled data sets to empirically determine that the false positives rate was low (Abiola *et al.* 2003). Pathway and network analysis was performed using Ingenuity pathway analysis (IPA) (Kramer *et al.* 2014)

RNA interference in RAW264.7 cells

RNA interference (RNAi) assays were carried out as previously described (Alper *et al.* 2008; Yang *et al.* 2009; De Arras *et al.* 2014a). Briefly, small interfering RNAs (siRNAs) (Dharmacon, Lafayette, CO; pools of four siRNA duplexes/gene) were transfected into the mouse macrophage cell line RAW264.7 using the Amaxa Nucleofector Shuttle according to the manufacturer's instructions. Transfections were carried out in 96-well format using 200,000 cells/well and 2 μm siRNA. Thirty-six hours after siRNA transfection, LTA was added to a final concentration of 2.5 μg/ml LTA. Supernatant was collected 5 hr post-LTA treatment, and cytokine production was assayed using DuoSet ELISA kits (R&D Systems). In experiments monitoring the response to lipopolysaccharide (LPS) instead of LTA, LPS was added at a final concentration of 20 ng/ml (LPS from List Biological Laboratories, Campbell, CA). Cell viability was monitored and cell number normalized using fluorescein diacetate as described (Fernandez-Botran and Vt'vička 2001; Alper *et al.* 2008). Cytokine production was normalized relative to a negative control siRNA (nontargeting siRNA, Dharmacon). RNA was isolated using the RNAEasy kit (QIAGEN, Valencia, CA) and the extent of gene knockdown was monitored by real-time (RT)-PCR with Taqman gene expression assays on an ABI Viia7 Real-Time PCR System (Applied Biosystems, Foster City, CA). The 384-well plate for qPCR was set up using the Freedom EVO robot (Tecan). siRNAs were initially tested in quadruplicate and siRNAs that affected cytokine production were further tested by transfecting each siRNA duplex in the pool individually to verify that multiple siRNAs targeting each gene could still induce the same phenotype. One-group two-tailed *t*-tests for siRNA data (testing for deviation

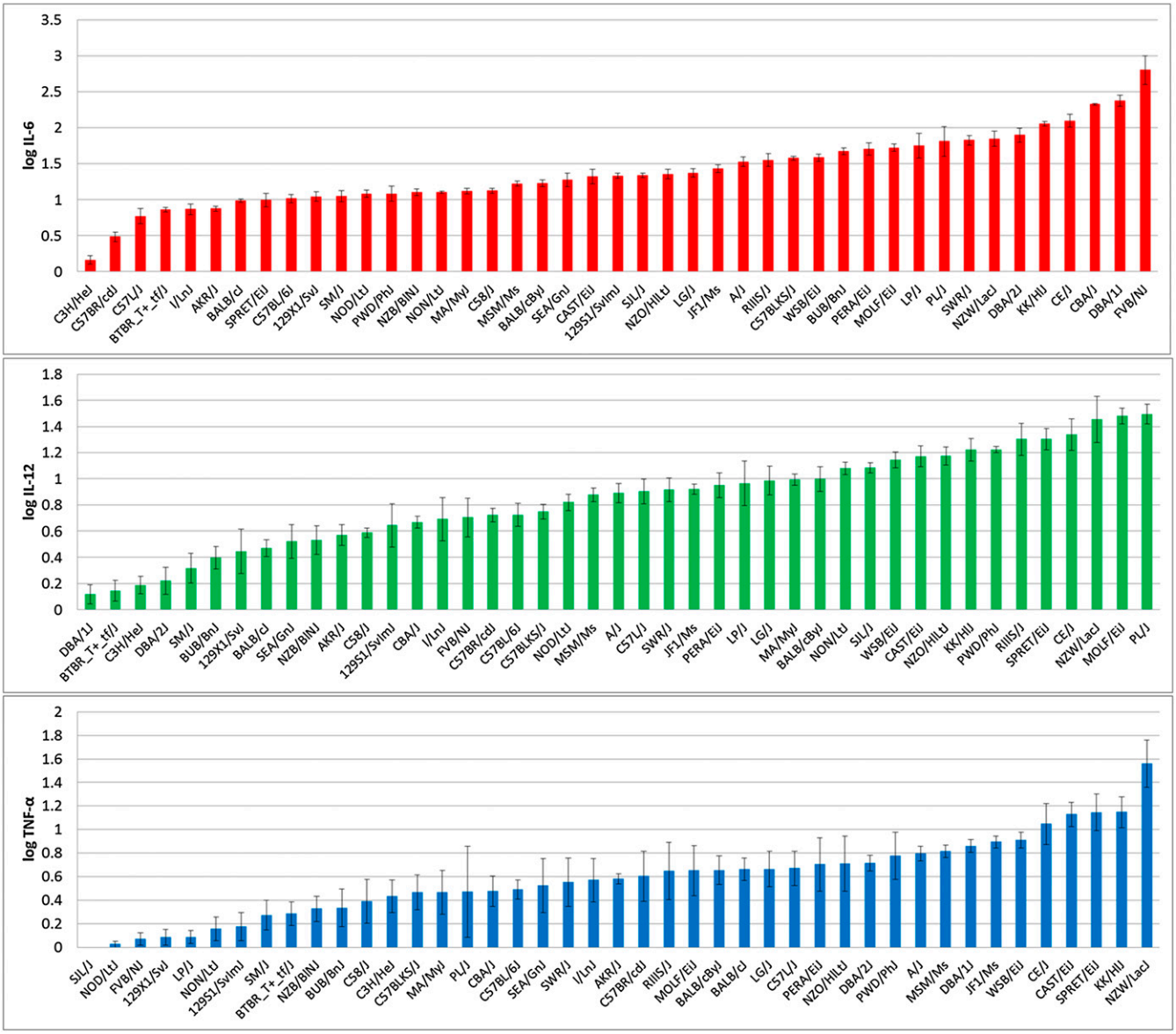

Figure 1 Post-LTA stimulation concentrations of IL-6 (top, red bars), IL-12 (middle, green bars), and TNF-α (bottom, blue bars) secreted by BMMs from 43 inbred mouse strains of mice. BMMs were stimulated with 0.5 μg/ml LTA for 5 hr and cytokine concentrations in the supernatant were measured by ELISA. In all three panels, means of three biological replicates with error bars representing SEMs are plotted.

from 1) and two-group unpaired two-tailed *t*-tests for qPCR data were performed in GraphPad Prism.

Gene overexpression in RAW264.7 cells

Plasmids containing full-length complementary DNAs (cDNAs) with stop codon cloned downstream of the cytomegalovirus (CMV) promoter were obtained for *Nkx6.1* (Origene); *Bdkrb1* (clone ID: 4753410), *Blnk* (clone ID: 5213221), and *Fbxo17* (clone ID: 4486850) (Open Biosystems), and negative control chloramphenicol acetyltransferase (CAT) (Invitrogen). Transient transfections were performed as previously described (De Arras *et al.* 2014b). Briefly, 100,000 cells plated in 24-well format were transfected with 3.75 μl Fugene HD (Roche), 300 ng NF-κB-AP1-luc (a derivative of the IL-8 promoter) (Mukaida *et al.* 1989), 100 ng SV40-rluc (Promega, Madison, WI), and 600 ng of overexpression plasmid. Twenty-four hours after transfection, cells were stimulated with LTA for 6 hr and then luciferase activity was monitored using the Dual Luciferase Assay Kit (Promega) using SV40-rluc as a normalization control for transfection efficiency. Unpaired two-group two-tailed *t*-tests were performed in GraphPad Prism.

Bdkrb1- and Bdkrb2-deficient BMMs

BMMs from *Bdkrb1*-deficient mice were stimulated with either LTA for 5 hr, heat-killed *S. pneumoniae* (HKSP) (Invivogen) for 18 hr, or heat-killed *S. aureus* (HKSA) (Invivogen) for 18 hr, and IL-6 and TNF-α in the supernatant were measured using

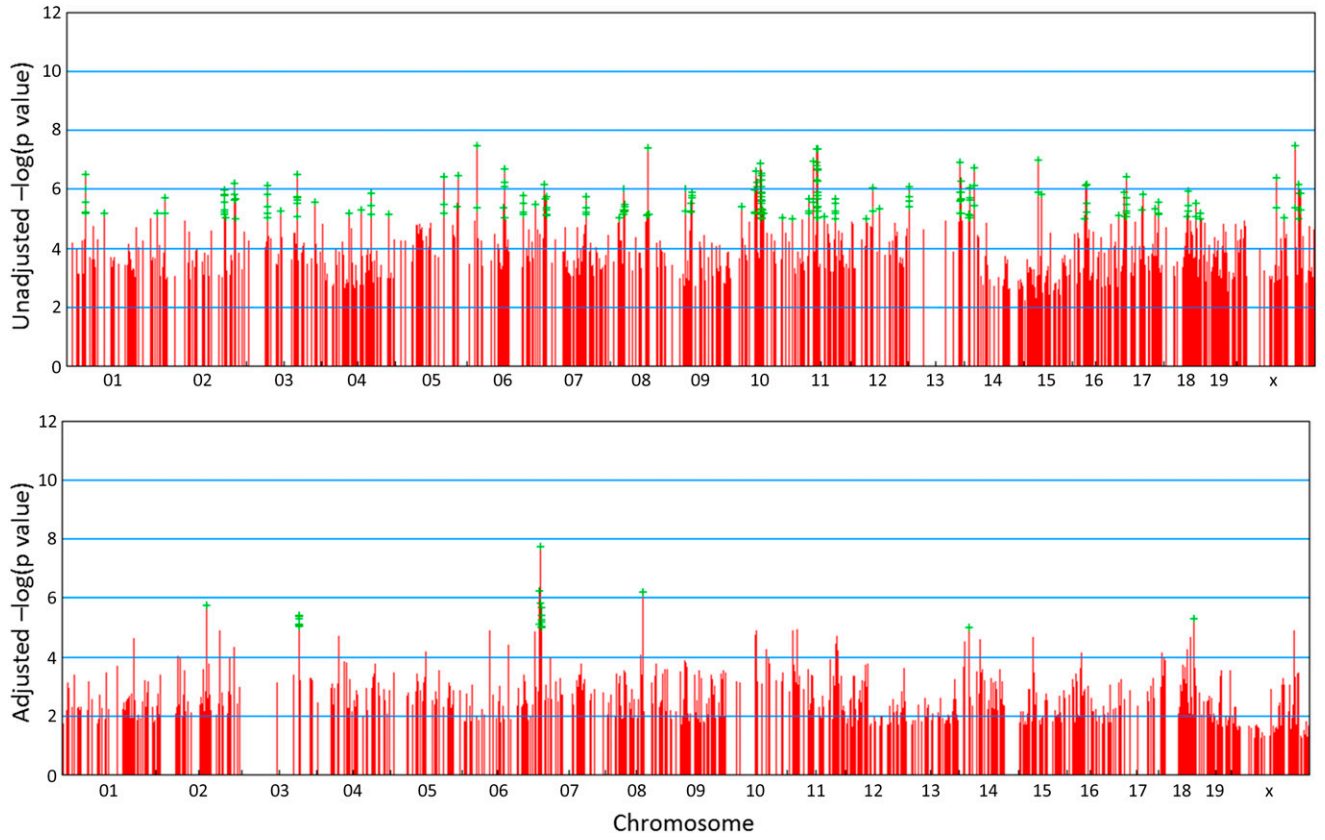

Figure 2 WGA mapping analysis of IL-12 produced by BMMs from 43 strains of mice in response to LTA stimulation. Top plot shows unadjusted *P*-values while bottom plot shows *P*-values after adjustment for relatedness among inbred strains of mice. Green plus symbols designate SNPs significantly associated with LTA-induced IL-12 production.

DuoSet ELISA kits (R&D Systems). ANOVAs with post hoc Tukey tests were performed in GraphPad Prism.

Data availability

The authors state that all data necessary for confirming the conclusions presented in the article are represented fully within the article.

Results

Use of inbred mouse strains to identify candidate regulators of the response to LTA

To investigate the differential response of macrophages to TLR2 stimulation, BMMs from 43 inbred strains of mice were stimulated with three concentrations of LTA (10.0, 0.5, and 0.025 μg/ml). To improve the diversity of the genetic background, eight wild-derived strains were included (Supplemental Material, Table S1) (Kirby *et al.* 2010). Concentrations of IL-6, IL-12, and TNF-α 5 hr post-treatment revealed significant variability in response among the 43 strains. The D'Agostino–Pearson omnibus normality test of log-transformed cytokine concentrations showed the most normal distribution of cytokine response to 0.5 μg/ml LTA stimulation with TNF-α response deviating most from a normal distribution (Table S2). The cytokine response induced by 0.5 μg/ml LTA stimulation across all 43 strains (Figure 1) was chosen for further analyses. To confirm the stability of these phenotypes, six strains of mice (C3H/HeJ, BALB/cByJ, C57BL/6J, DBA/1J, DBA/2J, and SJL/J) were rephenotyped in a separate set of experiments and similar cytokine concentrations with the same ranking of the strains as in the initial screen were observed (data not shown).

To identify genetic loci associated with cytokine response to LTA stimulation, we performed *in silico* WGA mapping on cytokine response to 0.5 μg/ml LTA stimulation. We used the EMMA algorithm developed by Kang *et al.* (2008) because it implements a genetic similarity matrix and a phylogenetic control method to account for population structure among inbred strains of mice, thereby limiting false positive associations (Kang *et al.* 2008), and we have successfully used it in our previous studies of innate immunity (Yang *et al.* 2009). The reduction in the false positive associations achieved by implementing the EMMA algorithm to perform WGA mapping of the IL-12 cytokine response data are depicted in Figure 2, A and B, demonstrating the appropriateness of this mapping approach in our study.

To identify genes in the loci significantly associated with the cytokine response to LTA stimulation, we determined loci boundaries by extending from the most significant single nucleotide polymorphism (SNP) in the analysis to encompass

Table 1 One-hundred seventeen loci identified as associated with IL-6, IL-12, and TNF-α response of macrophages to LTA by EMMA mapping

Cytokine	Chr	Start (bp)	End (bp)	Locus size (bp)
IL-6	chr1	173,660,282	173,660,282	
IL-6	chr1	174,635,407	174,681,425	46,018
IL-6	chr1	182,983,026	183,092,082	109,056
IL-6	chr13	83,926,870	84,019,016	92,146
IL-6	chr15	26,473,491	26,485,688	12,197
IL-6	chr18	75,055,572	75,055,572	
IL-6	chr18	76,434,758	76,444,590	9,832
IL-6	chr19	6,607,389	6,684,068	76,679
IL-6	chr19	6,896,895	6,931,773	34,878
IL-6	chr19	7,417,909	7,626,585	208,676
IL-6	chr19	8,039,764	8,527,516	487,752
IL-6	chr19	8,753,215	8,753,215	
IL-6	chr3	63,804,619	63,993,407	188,788
IL-6	chr3	139,773,695	139,929,431	155,736
IL-6	chr3	141,191,857	141,645,185	453,328
IL-6	chr3	141,768,183	141,823,620	55,437
IL-6	chr7	81,032,677	81,075,445	42,768
IL-6	chr8	90,554,504	90,554,504	
IL-6	chr8	117,778,948	117,778,948	
IL-6	chr8	126,224,093	126,252,702	28,609
IL-12	chr14	20,435,777	20,515,227	79,450
IL-12	chr7	13,302,434	13,302,434	
IL-12	chr7	14,954,483	15,009,969	55,486
IL-12	chr7	16,857,086	17,227,229	370,143
IL-12	chr8	79,136,882	79,436,459	299,577
TNF-α	chr1	39,035,119	39,181,313	146,194
TNF-α	chr1	173,661,396	173,884,837	223,441
TNF-α	chr10	50,611,055	50,611,055	
TNF-α	chr10	50,740,158	50,788,326	48,168
TNF-α	chr10	50,917,983	51,023,999	106,016
TNF-α	chr10	51,135,297	51,941,442	806,145
TNF-α	chr10	52,575,330	52,782,128	206,798
TNF-α	chr10	52,895,811	52,977,368	81,557
TNF-α	chr10	53,086,073	53,239,257	153,184
TNF-α	chr10	68,010,641	68,393,947	383,306
TNF-α	chr10	125,401,945	125,908,958	507,013
TNF-α	chr11	11,674,761	11,742,868	68,107
TNF-α	chr11	47,168,225	47,168,244	19
TNF-α	chr11	72,932,205	74,484,806	1,552,601
TNF-α	chr11	87,114,852	87,158,145	43,293
TNF-α	chr11	90,096,091	90,274,475	178,384
TNF-α	chr11	101,977,726	103,331,421	1,353,695
TNF-α	chr12	5,260,013	5,591,949	331,936
TNF-α	chr12	45,440,710	47,752,680	2,311,970
TNF-α	chr12	106,725,372	106,879,407	154,035
TNF-α	chr12	108,031,321	108,249,927	218,606
TNF-α	chr12	108,381,002	108,424,555	43,553
TNF-α	chr13	40,553,224	40,770,110	216,886
TNF-α	chr14	29,545,056	29,545,056	
TNF-α	chr14	33,768,861	34,187,798	418,937
TNF-α	chr14	80,516,031	80,781,218	265,187
TNF-α	chr16	51,934,234	51,957,839	23,605
TNF-α	chr16	52,796,410	53,140,991	344,581
TNF-α	chr18	46,359,998	46,369,259	9,261
TNF-α	chr18	61,292,691	61,715,155	422,464
TNF-α	chr18	63,484,322	6,3941,799	457,477
TNF-α	chr18	77,580,880	7,7819,968	239,088
TNF-α	chr19	6,045,940	6,045,940	
TNF-α	chr19	40,915,624	41,163,200	247,576
TNF-α	chr19	41,960,523	42,173,169	212,646
TNF-α	chr2	136,181,592	138,515,186	2,333,594
TNF-α	chr2	143,850,108	143,850,108	
TNF-α	chr2	163,054,911	163,298,162	243,251
TNF-α	chr3	4,126,466	5,309,431	1,182,965
TNF-α	chr3	39,534,158	41,662,341	2,128,183
TNF-α	chr3	41,811,467	43,139,599	1,328,132
TNF-α	chr3	44,572,664	46,423,886	1,851,222
TNF-α	chr3	46,532,654	47,266,354	733,700
TNF-α	chr3	50,825,016	52,618,750	1,793,734
TNF-α	chr3	83,640,855	83,846,453	205,598
TNF-α	chr3	157,306,420	157,402,557	9,6137
TNF-α	chr4	7,064,861	7,528,602	463,741
TNF-α	chr4	31,169,777	31,331,142	161,365
TNF-α	chr4	65,675,157	66,157,867	482,710
TNF-α	chr4	79,461,643	80,868,868	1407,225
TNF-α	chr4	103,305,852	103,464,317	158,465
TNF-α	chr4	103,728,271	103,902,841	174,570
TNF-α	chr4	104,241,765	104,336,024	94,259
TNF-α	chr4	143,774,477	143,945,145	170,668
TNF-α	chr5	83,480,859	83,768,222	287,363
TNF-α	chr5	102,050,296	102,259,957	209,661
TNF-α	chr5	102,450,545	102,554,777	104,232
TNF-α	chr5	114,170,021	114,364,985	194,964
TNF-α	chr5	114,660,785	114,768,095	107,310
TNF-α	chr5	128,332,778	128,341,406	8,628
TNF-α	chr5	133,935,870	134,009,002	73,132
TNF-α	chr6	21,142,574	21,313,770	171,196
TNF-α	chr6	30,290,830	30,462,108	171,278
TNF-α	chr6	30,665,722	30,671,396	5,674
TNF-α	chr6	31,059,957	31,239,548	179,591
TNF-α	chr6	79,494,699	80,577,083	1082,384
TNF-α	chr6	81,472,746	81,657,303	184,557
TNF-α	chr6	110,841,305	111,262,820	421,515
TNF-α	chr6	111,442,758	112,271,201	828,443
TNF-α	chr6	130,938,748	131,015,928	77,180
TNF-α	chr7	82,755,139	83,269,370	514,231
TNF-α	chr7	141,656,566	141,774,343	117,777
TNF-α	chr8	72,748,804	72,748,804	
TNF-α	chr9	22,482,848	22,482,848	
TNF-α	chr9	30,770,731	31,702,031	931,300
TNF-α	chr9	42,207,980	42,490,846	282,866
TNF-α	chr9	85,402,341	85,477,102	74,761
TNF-α	chr9	93,775,695	97,653,544	3,877,849
TNF-α	chr9	109,384,502	109,707,867	323,365
TNF-α	chrX	96,138,670	96,211,687	73,017
TNF-α	chrX	112,462,964	112,494,950	31,986
TNF-α	chrX	122,722,705	122,831,118	108,413
TNF-α	chrX	122,949,728	123,652,382	702,654
TNF-α	chrX	122,949,728	123,652,382	
TNF-α	chrX	124,009,011	124,073,705	64,694
TNF-α	chrX	124,193,246	124,340,106	146,860
TNF-α	chrX	124,477,770	124,800,822	323,052
TNF-α	chrX	124,906,257	125,118,241	211,984
TNF-α	chrX	126,116,468	126,148,778	32,310
TNF-α	chrX	126,389,225	126,798,587	409,362
TNF-α	chrX	131,417,076	131,646,505	229,429
TNF-α	chrX	131,771,131	131,871,707	100,576

(continued)

Table 1, *continued*

all linked SNPs with $P < 1 \times 10^{-4}$. This resulted in 20 loci (average locus size = 0.133 Mb; 18 known genes) for the IL-6 response, 5 loci (0.201 Mb average; 7 known genes) for the IL-12 response, and 92 loci (0.464 Mb average; 186 known

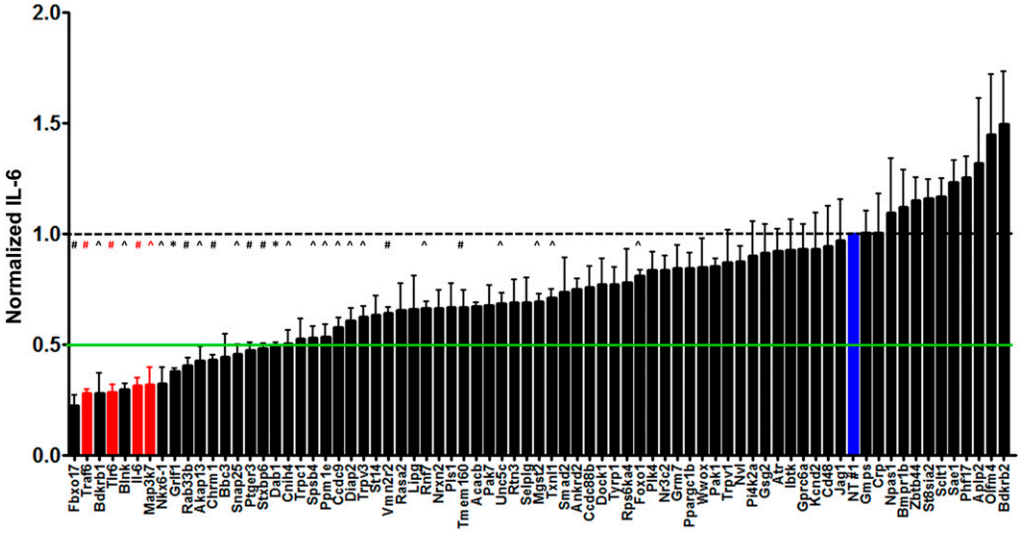

Figure 3 The effect of RNAi-mediated inhibition of 71 genes from WGA mapping in RAW264.7 macrophages on LTA-induced IL-6 production. Pools of four siRNA duplexes per gene were transfected into RAW264.7 cells, LTA was added, and cytokine production was monitored. Shown are the results for negative control siRNA (blue; nontargeting siRNA from Dharmacon), four positive control siRNAs (red; Traf6, Tlr6, Il-6, and Map3k7), and 71 siRNAs targeting genes identified by our eQTL mapping analysis (black). All data are normalized to the NT#1 nontargeting negative control siRNA. Means of four independent measurements with error bars representing SEMs are plotted; green line indicates threshold for twofold reduction in IL-6 response as a result of gene inhibition. $^{*}P < 0.0001$, $^{\#}P < 0.001$, and $^{\wedge}P < 0.01$ by one-group two-tailed *t*-test testing for deviation from 1.

genes) for the TNF-α response (Table 1 and Table S3). The resolution of mapping is poorer (loci are larger), and there are more significant associations for TNF-α production due to the larger deviations from normality compared to IL-6 or IL-12 production. To prioritize genes in the TNF-α response loci for further studies, we performed a systems analysis using IPA. The two top-scoring protein–protein interaction networks identified by IPA contain 46 of the 186 genes that mapped to the TNF-α response (Figure S1). The top network (score = 42) centers on NF-κB, p38 MAPK, and TGF-β while hubs in the second network (score = 36) consist of several kinases (PI3K, ERK1/2, PKA, and PKC), demonstrating the relevance of these networks to the innate immune response (Fukao and Koyasu 2003; Takeuchi and Akira 2010).

We also performed 10 permutations with shuffled data sets to confirm a low false positive rate in EMMA mapping. We observed only one false positive in 1 of the 10 permutations for IL-6 response, no associations for IL-12 response, and one false positive in three of the 10 permutation for TNF-α response.

Use of RNAi to prioritize candidate genes

Our analysis identified a total of 71 high-priority candidate genes (18 IL-6, 7 IL-12, and 46 TNF-α + pathway) that are likely to be important in the innate immune response to LTA (Table S4). To functionally test the potential role of the 71 candidate genes identified by our analysis, we used RNAi to inhibit each of these genes in the RAW264.7 mouse macrophage cell line and monitored the resulting effect on LTA-induced IL-6 production. A pool of four siRNA duplexes targeting each gene was transfected into the macrophages, the cells were exposed to LTA, and 5 hr later, cytokines secreted into the supernatant were analyzed by ELISA. As a control, we demonstrated that LTA-induced IL-6 production was decreased when known LTA response genes were inhibited (*Tlr6*, *Traf6*, *IL-6*, and *Map3k7*) (Figure 3). RNAi-mediated inhibition of 8 of the 71 candidate genes (*Fbxo17*, *Bdkrb1*, *Blnk*, *Nkx6-1*, *Grif1*, *Rab33b*, *Akap13*, and *Chrm1*) resulted in a more than twofold reduction in IL-6 production in response to LTA stimulation (Figure 3). In contrast, IL-6 production was moderately increased when *Bdkrb2*, a gene closely related to Bdkrb1, was inhibited (Figure 3).

To confirm that these RNAi treatments were inhibiting the corresponding endogenous gene, we used Taqman gene expression assays to monitor expression of all nine genes whose inhibition resulted in changes in IL-6 production in response to LTA (the eight genes whose inhibition weakened the LTA response: *Fbxo17*, *Bdkrb1*, *Blnk*, *Nkx6-1*, *Grif1*, *Rab33b*, *Akap13*, *Chrm1*, and the one gene whose inhibition increased the response: *Bdkrb2*) (Figure S2). siRNA treatment results in a >2-fold inhibition of gene expression for each gene compared to nontargeting siRNA control, except for Nkx6-1 RNAi, which decreased Nkx6-1 expression 1.8-fold. Comparison of normalized expression levels (ΔCt values) in siRNA targeted cells compared to the nontargeting siRNA pool demonstrated a significant reduction in expression (unpaired two-tailed test $P < 0.01$) for all genes except for Nkx6-1.

To confirm that the effects of these RNAi treatments were due to inhibition of the corresponding endogenous genes and not due to an off-target RNAi effect, we inhibited each of the nine genes whose inhibition resulted in changes in IL-6 production in response to LTA with four independent siRNA duplexes targeting each gene. At least two of the individual siRNA duplexes resulted in a more than twofold reduction in IL-6 production in response to LTA for four (*Fbxo17*, *Bdkrb1*, *Blnk*, and *Nkx6-1*) of the nine genes tested (Figure 4). This is consistent with the effect of these RNAi treatments being due to inhibition of that specific target gene. Taken together, these siRNA data support the potential role of Fbxo17, Bdkrb1, Blnk, and Nkx6-1 in the macrophage response to LTA.

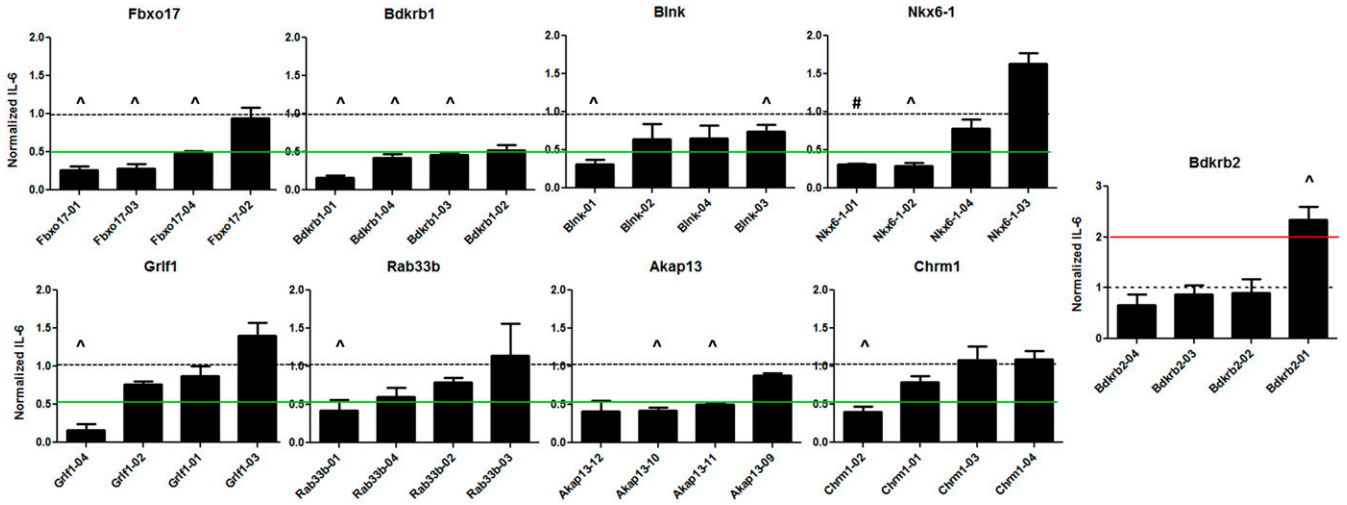

Figure 4 The effect of individual siRNA duplexes for nine candidate genes from the siRNA screen in RAW264.7 macrophages on LTA-induced IL-6 production. Four siRNA duplexes were transfected individually for each of the eight genes whose inhibition resulted in decreased IL-6 production and one gene whose inhibition resulted in higher IL-6 production in the screen presented in Figure 3. Means of four independent measurements with error bars representing SEMs are plotted; green lines indicate threshold for twofold reduction and red twofold increases in IL-6 response as a result of gene inhibition. $^{\#}P < 0.001$ and $^{\wedge}P < 0.01$ by one-group two-tailed *t*-test testing for deviation from 1.

The effect of these four genes was not unique to the macrophage response to LTA. Inhibition of Fbxo17, Bdkrb1, Blnk, and Nkx6-1 using RNAi also greatly weakened IL-6 production induced by the TLR4 agonist LPS (Figure S3). Thus, these four genes are required for a robust innate immune response induced by both Gram positive (LTA) and Gram negative (LPS) bacterial stimuli.

Use of gene overexpression to verify the innate immune regulatory function of candidate genes

RNAi-mediated inhibition of *Fbxo17*, *Bdkrb1*, *Blnk*, and *Nkx6-1* led to a weakened response to LTA. To further test the effects of these gene candidates, we overexpressed full-length cDNAs of each gene and monitored the effect using an innate immunity-responsive luciferase reporter. If overexpression induced a phenotype opposite to the RNAi-induced phenotype, that would support a role of that gene in innate immunity regulation. In contrast, lack of an overexpression phenotype is not necessarily indicative of gene function.

To determine whether overexpression of these four candidate genes led to a more pronounced innate immune response to LTA, we transiently overexpressed each of *Fbxo17*, *Bdkrb1*, *Blnk*, and *Nkx6-1* using full-length cDNA clones under control of the CMV promoter, stimulated cells with LTA, and monitored innate immune activation using a NF-κB-AP1-luciferase reporter. As a negative control, cells were transfected with a plasmid overexpressing CAT, which should not alter innate immunity. Overexpression of all four candidate genes tested led to increased NF-κB-AP1 activity (Figure 5), a phenotype opposite to that caused by inhibition of these genes. Thus, these gain-of-function data provide evidence that the wild-type function of these four genes is to amplify the innate immune response induced by LTA.

BMM Bdrkb1-deficient mice exhibit a weakened response to Gram negative stimuli

To further verify some of the results from our genetic studies and elucidate the role of Bdkrb1 in the macrophage response to Gram positive bacteria, we exposed BMMs from *Bdkrb1*-deficient mice (Pesquero *et al.* 2000) to LTA, HKSP, or HKSA, and monitored resulting inflammatory cytokine production. *Bdkrb1*-deficient macrophages produce little or no IL-6 or TNF-α when challenged with LTA (for 5 hr) compared to control macrophages from wild-type mice (Figure 6, A and B). These data are consistent with the RNAi and overexpression studies, although complete knockout of Bdrkb1, as expected, induced a much stronger phenotype than RNAi-mediated partial knockdown.

Eighteen hours post-HKSA stimulation, *Bdkrb1*-deficient macrophages also produce less IL-6 and TNF-α than wild-type macrophages (Figure 6, C and D). In contrast, HKSP stimulation of *Bdkrb1*-deficient macrophages resulted in similar or enhanced cytokine production compared to wild-type control macrophages (Figure 6, C and D), demonstrating the complexity of the response. These data further support the importance of *Bdkrb1* in macrophages response to Gram positive bacterial stimulation but also underscore the complexity of this response given the differences in response to HKSP and HKSA.

Discussion

Using a combination of WGA mapping in inbred strains of mice, pathway analysis, and analysis of gene function in cell lines, we have identified specific genes and loci that regulate the macrophage response to LTA, a component of the cell wall of Gram positive bacteria. Four genes (*Bdkrb1*, *Blnk*, *Fbxo17*,

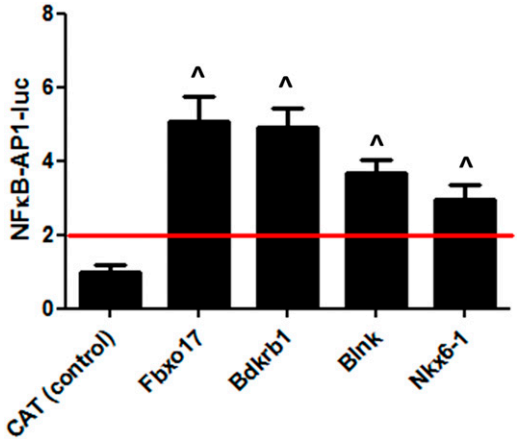

Figure 5 Effect of overexpression of four target genes in RAW264.7 cells on NF-κB activation. Plasmids containing full-length cDNAs for the indicated genes (or CAT negative control) cloned downstream of the CMV promoter were cotransfected with NF-kB-AP1-luc and SV40-rluc plasmids. Following transfection, cells were stimulated with 2.5 μg/ml LTA for 5 hr, and innate immune responsiveness was monitored by measuring luciferase production. Means of three independent measurements with error bars representing SEMs are plotted, and red line indicates threshold for twofold increase in IL-6 response as a result of gene overexpression. Compared to CAT (set to 1), $^P < 0.01$ by unpaired two-group two-tailed *t*-test.

and *Nkx6-1*) emerged from our analysis as high priority candidates due to changes in macrophage response to LTA as a result of their inhibition and overexpression in cell culture. Moreover, we validated the loss- and gain-of-function strategies to identify novel regulators of the response to LTA by demonstrating that Bdkrb1-deficient macrophages were less responsive to LTA and HKSA. Interestingly, all four genes identified in this study also regulated the response to the Gram negative bacterial component LPS, suggesting that these genes may have a more general role in TLR signaling.

Bradykinin 1 receptor (*Bdkrb1*) has a well-established role in the regulation of inflammation, particularly in the brain (Albert-Weissenberger *et al.* 2014), cardiovascular system (Couture *et al.* 2014), and the lung (Yang *et al.* 2014). Bradykinin receptor genes encode two G-protein-coupled receptors, inducible BDKRB1, and constitutive BDKRB2, that respond to endogenous kinin ligands as well as cytokines via the NF-κB pathway in the case of inducible BDKRB1 (Couture *et al.* 2014). Both bradykinin receptors were identified in the TNF-α response to LTA in our mapping study. *Bdkrb1* gene inhibition led to decreased and *Bdkrb2* gene inhibition to increased cytokine production in response to LTA stimulation in cultured macrophages, consistent with the complementary roles of these two receptors (Couture *et al.* 2014). Our study is the first to demonstrate a role for kinin receptors in the response to Gram positive bacterial stimulation. Interestingly, *Bdkrb1*-deficient macrophages produced less TNF-α in response to LTA and HKSA but more in response to HKSP, suggesting that other PAMPs may be important in this response.

The *Blnk* gene (also known as BASH or SLP-65 in mice) (Hayashi *et al.* 2000) has not been implicated in regulating innate immunity previously, although it is known to regulate the immune system. *Blnk* encodes a cytoplasmic linker protein that plays a critical role in B-cell development (Jumaa *et al.* 1999; Pappu *et al.* 1999). This protein mediates IL-10 production in regulatory B-cells and thus limits the allergic and autoimmune response (Jin *et al.* 2013). It is expressed by macrophages (Bonilla *et al.* 2000) and plasmacytoid dendritic cells (pDCs) (Marafioti *et al.* 2008). *Blnk* was identified in the TNF-α response to LTA in our mapping study, suggesting a potential role in host response to Gram positive infection. Our RNAi and cDNA overexpression studies indicate that wild-type *Blnk* is a positive effector of the response to LTA in mouse macrophages.

Fbxo17 encodes a member of the F-box family of proteins, one of the four subunits of the ubiquitin protein ligase complex SCFs (SKP1-cullin-F-box), which function in phosphorylation-dependent ubiquitination, a crticial step in TLR signaling pathways (Takeuchi and Akira 2010). While other members of this gene family have been implicated in the regulation of immunity previously, *Fbxo17* has not. Inhibition of another member of this protein family, FBXO3, led to a decreased cytokine response in multiple animal models, suggesting a critical role in the regulation of inflammation (Chen *et al.* 2013). Our earlier WGA mapping study in mice demonstrated that another member of this protein family, FBXO9, plays a role in the host response to LPS (Yang *et al.* 2009). Identification of *Fbxo17* as associated with IL-6 production by macrophages in response to LTA in the present study provides further support for the role of this protein family in innate immunity and provides the first evidence of its potential importance in the response to Gram positive organisms. Our studies indicate that wild-type *Blnk* is a positive effector of the response to LTA in mouse macrophages.

Nkx6-1 is a member of the NK homeobox transcription factor gene family that plays an important role in development. *Nkx6-1* is specifically required for the development of β-cells in the pancreas (Inoue *et al.* 1997), but it has no known role in immunity and inflammation. Therefore, our data demonstrating that *Nkx6-1* is associated with TNF-α response of macrophages to LTA provide the first evidence for its potential role in innate immunity. Given its role in the development, it is possible that this transcription factor plays a role in the development of the innate immune system, but the pathway and specificity of response to LTA require further investigation. Our studies do demonstrate that *Nkx6-1* is a positive regulator of the response induced by LTA in fully differentiated macrophages.

There are several limitations to our study. First, we only mapped the macrophage response to LTA in inbred strains of mice; additional mapping of response to other Gram positive PAMPs, such as peptidoglycan, would provide a more comprehensive view of the macrophage response to Gram positive bacteria. Second, by using a PAMP instead of heat-killed

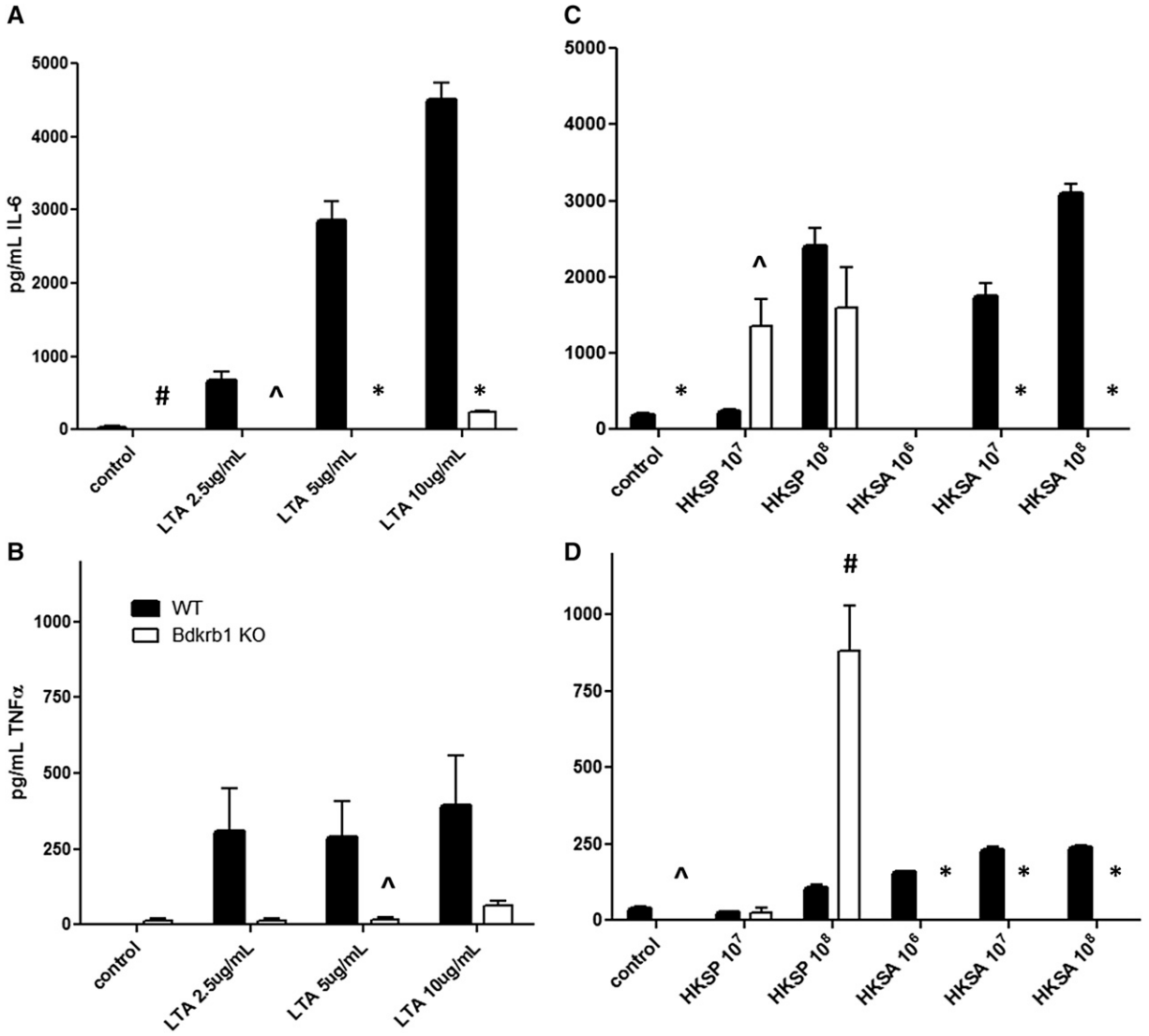

Figure 6 Effect of Bdkrb1 gene deletion on the macrophage response to Gram positive bacterial stimulation. Depicted are IL-6 (A and C) and TNF-α (B and D) production by Bdkrb1-deficient or wild-type macrophages following stimulation with LTA (A and B), HSKP (C and D), or HKSA (C and D). In all panels, means of three to eight biological replicates with error bars representing SEMs are plotted. $^{*}P < 0.0001$, $^{\#}P < 0.001$, and $^{\wedge}P < 0.01$ by two-group unpaired two-tailed *t*-test between Bdkrb1-deficient and wild-type macrophages.

and live bacteria, we likely did not capture the complexity of macrophage response to multiple PAMPs. Third, our siRNA screen was performed only in one cell line; additional cell lines and primary cells would provide additional evidence for a functional role of specific gene candidates. An important future direction of our work will be to test the effect of Bdkrb1 deletion on *in vivo* susceptibility to *S. aureus* infection.

Gram positive bacteria are a common cause of pneumonia, and in addition, *S. aureus* infections are common in hospital settings. These major public health issues will require further study of both host and microbial genetics to identify better and more tailored treatments for patients who become actively infected with Gram positive pathogens. The current study provides important insight into the host genetic basis of the innate immune response to Gram positive bacteria and provides candidate genes that warrant further study in model systems and human populations. We identified four innate immune response genes (*Bdkrb1*, *Blnk*, *Fbxo17*, and *Nkx6-1*) in our genetic studies that were validated in our RNAi and overexpression studies as genes that regulate the response to LTA. Additionally, we note that some of the other 71 genes identified in our genetic analysis may also contribute to Gram positive bacterial susceptibility, as negative siRNA results in one cell line do not completely rule out a gene's function in the innate immune response to LTA.

Acknowledgments

This work was funded by National Institutes of Health grants P01-ES18181 (D.A.S. and I.V.Y.), R21-ES019256 (S.A.), and P01-AI060699 (P.B.M.).

Literature Cited

Abiola, O., J. M. Angel, P. Avner, A. A. Bachmanov, J. K. Belknap *et al.*, 2003 The nature and identification of quantitative trait loci: a community's view. Nat. Rev. Genet. 4: 911–916.

Albert-Weissenberger, C., S. Mencl, S. Hopp, C. Kleinschnitz, and A. L. Siren, 2014 Role of the kallikrein-kinin system in traumatic brain injury. Front. Cell. Neurosci. 8: 345.

Alper, S., R. Laws, B. Lackford, W. A. Boyd, P. Dunlap *et al.*, 2008 Identification of innate immunity genes and pathways using a comparative genomics approach. Proc. Natl. Acad. Sci. USA 105: 7016–7021.

Bonilla, F. A., R. M. Fujita, V. I. Pivniouk, A. C. Chan, and R. S. Geha, 2000 Adapter proteins SLP-76 and BLNK both are expressed by murine macrophages and are linked to signaling via Fcγ receptors I and II/III. Proc. Natl. Acad. Sci. USA 97: 1725–1730.

Brouwer, M. C., J. de Gans, S. G. Heckenberg, A. H. Zwinderman, T. van der Poll *et al.*, 2009 Host genetic susceptibility to pneumococcal and meningococcal disease: a systematic review and meta-analysis. Lancet Infect. Dis. 9: 31–44.

Chen, B. B., T. A. Coon, J. R. Glasser, B. J. McVerry, J. Zhao *et al.*, 2013 A combinatorial F box protein directed pathway controls TRAF adaptor stability to regulate inflammation. Nat. Immunol. 14: 470–479.

Couture, R., N. Blaes, and J. P. Girolami, 2014 Kinin receptors in vascular biology and pathology. Curr. Vasc. Pharmacol. 12: 223–248.

De Arras, L., B. S. Guthrie, and S. Alper, 2014a Using RNA-interference to investigate the innate immune response in mouse macrophages. J. Vis. Exp. 3: e51306.

De Arras, L., R. Laws, S. M. Leach, K. Pontis, J. H. Freedman *et al.*, 2014b Comparative genomics RNAi screen identifies Eftud2 as a novel regulator of innate immunity. Genetics 197: 485–496.

Fernandez-Botran, R., and V. Vt'vička, 2001 *Methods in Cell Immunology*, CRC, Boca Raton, FL.

Fukao, T., and S. Koyasu, 2003 PI3K and negative regulation of TLR signaling. Trends Immunol. 24: 358–363.

Gingles, N. A., J. E. Alexander, A. Kadioglu, P. W. Andrew, A. Kerr *et al.*, 2001 Role of genetic resistance in invasive pneumococcal infection: identification and study of susceptibility and resistance in inbred mouse strains. Infect. Immun. 69: 426–434.

Hayashi, K., R. Nittono, N. Okamoto, S. Tsuji, Y. Hara *et al.*, 2000 The B cell-restricted adaptor BASH is required for normal development and antigen receptor-mediated activation of B cells. Proc. Natl. Acad. Sci. USA 97: 2755–2760.

Hollingsworth, J. W., G. Whitehead, K. G. Berman, E. M. Tekippe, M. I. Gilmour *et al.*, 2007 Genetic basis of murine antibacterial defense to streptococcal lung infection. Immunogenetics 59: 713–724.

Inoue, H., A. Rudnick, M. S. German, R. Veile, H. Donis-Keller *et al.*, 1997 Isolation, characterization, and chromosomal mapping of the human Nkx6.1 gene (NKX6A), a new pancreatic islet homeobox gene. Genomics 40: 367–370.

Jin, G., Y. Hamaguchi, T. Matsushita, M. Hasegawa, D. Le Huu *et al.*, 2013 B-cell linker protein expression contributes to controlling allergic and autoimmune diseases by mediating IL-10 production in regulatory B cells. J. Allergy Clin. Immunol. 131: 1674–1682.

Jumaa, H., B. Wollscheid, M. Mitterer, J. Wienands, M. Reth *et al.*, 1999 Abnormal development and function of B lymphocytes in mice deficient for the signaling adaptor protein SLP-65. Immunity 11: 547–554.

Kang, H. M., N. A. Zaitlen, C. M. Wade, A. Kirby, D. Heckerman *et al.*, 2008 Efficient control of population structure in model organism association mapping. Genetics 178: 1709–1723.

Kirby, A., H. M. Kang, C. M. Wade, C. Cotsapas, E. Kostem *et al.*, 2010 Fine mapping in 94 inbred mouse strains using a high-density haplotype resource. Genetics 185: 1081–1095.

Kramer, A., J. Green, J. Pollard, Jr., and S. Tugendreich, 2014 Causal analysis approaches in Ingenuity Pathway Analysis. Bioinformatics 30: 523–530.

Liu, L., S. Oza, D. Hogan, J. Perin, I. Rudan *et al.*, 2015 Global, regional, and national causes of child mortality in 2000–13, with projections to inform post-2015 priorities: an updated systematic analysis. Lancet 385: 430–440.

Marafioti, T., J. C. Paterson, E. Ballabio, K. K. Reichard, S. Tedoldi *et al.*, 2008 Novel markers of normal and neoplastic human plasmacytoid dendritic cells. Blood 111: 3778–3792.

Mukaida, N., M. Shiroo, and K. Matsushima, 1989 Genomic structure of the human monocyte-derived neutrophil chemotactic factor IL-8. J. Immunol. 143: 1366–1371.

Pappu, R., A. M. Cheng, B. Li, Q. Gong, C. Chiu *et al.*, 1999 Requirement for B cell linker protein (BLNK) in B cell development. Science 286: 1949–1954.

Pesquero, J. B., R. C. Araujo, P. A. Heppenstall, C. L. Stucky, J. A. Silva, Jr. *et al.*, 2000 Hypoalgesia and altered inflammatory responses in mice lacking kinin B1 receptors. Proc. Natl. Acad. Sci. USA 97: 8140–8145.

Shukla, S. K., W. Rose, and S. J. Schrodi, 2015 Complex host genetic susceptibility to *Staphylococcus aureus* infections. Trends Microbiol. 23: 529–536.

Takeuchi, O., and S. Akira, 2010 Pattern recognition receptors and inflammation. Cell 140: 805–820.

Ting, J. P., S. B. Willingham, and D. T. Bergstralh, 2008 NLRs at the intersection of cell death and immunity. Nat. Rev. Immunol. 8: 372–379.

van der Poll, T., and S. M. Opal, 2009 Pathogenesis, treatment, and prevention of pneumococcal pneumonia. Lancet 374: 1543–1556.

Weischenfeldt, J., and B. Porse, 2008 Bone marrow-derived macrophages (BMM): isolation and applications. CSH Protoc. 2008: pdb.prot5080.

Yang, I. V., C. M. Wade, H. M. Kang, S. Alper, H. Rutledge *et al.*, 2009 Identification of novel genes that mediate innate immunity using inbred mice. Genetics 183: 1535–1544.

Yang, I. V., S. Alper, B. Lackford, H. Rutledge, L. A. Warg *et al.*, 2011a Novel regulators of the systemic response to lipopolysaccharide. Am. J. Respir. Cell Mol. Biol. 45: 393–402.

Yang, I. V., W. Jiang, H. R. Rutledge, B. Lackford, L. A. Warg *et al.*, 2011b Identification of novel innate immune genes by transcriptional profiling of macrophages stimulated with TLR ligands. Mol. Immunol. 48: 1886–1895.

Yang, Y., N. Zhang, F. Lan, K. Van Crombruggen, L. Fang *et al.*, 2014 Transforming growth factor-beta 1 pathways in inflammatory airway diseases. Allergy 69: 699–707.

Zaas, A. K., G. Liao, J. W. Chien, C. Weinberg, D. Shore *et al.*, 2008 Plasminogen alleles influence susceptibility to invasive aspergillosis. PLoS Genet. 4: e1000101.

Communicating editor: D. W. Threadgill

GENETICS

Supporting Information
www.genetics.org/lookup/suppl/doi:10.1534/genetics.115.185314/-/DC1

Novel Innate Immune Genes Regulating the Macrophage Response to Gram Positive Bacteria

Scott Alper, Laura A. Warg, Lesly De Arras, Brenna R. Flatley, Elizabeth J. Davidson, Jenni Adams, Keith Smith, Christine L. Wohlford-Lenane, Paul B. McCray, Jr., Brent S. Pedersen, David A. Schwartz, and Ivana V. Yang

DOI: 10.1534/genetics.115.185314

Figure S1. Ingenuity Pathway Analysis of genes mapped to the TNF-α cytokine response. Shown are the two most significant networks (score=42 and 35). Gray symbols denote genes on the TNF-α gene list; white symbols denote genes in the network but not on the gene list. (.tif, 742 KB)

Available for download as a .tif file at:

http://www.genetics.org/lookup/suppl/doi:10.1534/genetics.115.185314/-/DC1/FigureS1.tif

Figure S2. Fold change for expression of siRNA target genes in siRNA-treated compared to nontargeting control-treated RAW264.7. Data were analyzed using relative expression ΔΔCt method using GAPDH as the housekeeping gene. Plotted are means with SEM for four biological replicate experiments. (.tif, 54 KB)

Available for download as a .tif file at:

http://www.genetics.org/lookup/suppl/doi:10.1534/genetics.115.185314/-/DC1/FigureS2.tif

Figure S3. The effect of RNAi-mediated inhibition of four candidate genes in RAW264.7 macrophages on LPS-induced IL-6 production. Pools of four siRNA duplexes per gene were transfected into RAW264.7 cells, LPS was added, and cytokine production was monitored. Shown are the results for negative control siRNA (nontargeting siRNA from Dharmacon), positive control siRNA targeting the LPS receptor TLR4 , and 4 siRNA pools targeting candidate genes that are required for the response to LTA. *p<0.0001, #p<0.001, ^p<0.01 by one group two-tailed t-test testing for deviation from 1. (.tif, 968 KB)

Available for download as a .tif file at:

http://www.genetics.org/lookup/suppl/doi:10.1534/genetics.115.185314/-/DC1/FigureS3.tif

Table S1. List of 43 inbred mouse strains and Jackson Labs stock number. (.xlsx, 15 KB)

Available for download as a .xlsx file at:

http://www.genetics.org/lookup/suppl/doi:10.1534/genetics.115.185314/-/DC1/TableS1.xlsx

Table S2. Examination of normality of log-transformed cytokine concentrations on response to three concentrations of LTA. (.xlsx, 14 KB)

Available for download as a .xlsx file at:

http://www.genetics.org/lookup/suppl/doi:10.1534/genetics.115.185314/-/DC1/TableS2.xlsx

Table S3. Loci identified as associated with IL-6, IL-12, or TNF-a response of macrophages to LTA by EMMA mapping. (.xlsx, 27 KB)

Available for download as a .xlsx file at:

http://www.genetics.org/lookup/suppl/doi:10.1534/genetics.115.185314/-/DC1/TableS3.xlsx

Table S4. 71 genes within genomic loci identified by EMMA mapping of cytokines (IL-6, IL-12, and TNF-α) secreted by BMDMs from 43 strains of mice in response to LTA stimulation. TNF- α genes were prioritized using network analysis of all 186 genes. (.xlsx, 22 KB)

Available for download as a .xlsx file at:

http://www.genetics.org/lookup/suppl/doi:10.1534/genetics.115.185314/-/DC1/TableS4.xlsx